

Quantum Mechanical Analysis on Faujasite-Type Molecular Sieves by Using Fermi Dirac Statistics and Quantum Theory of Dielectricity

¹SALMA JABEEN*, ¹SYED MOHSIN RAZA, ¹M. ASHFAQ AHMED, ²MASOOM YASEEN ZAI,
³SHER AKBAR AND ⁴YASMIN ZAHRA JAFRI

¹Department of Physics, University of Balochistan, Sariab road Quetta- 87300, Pakistan.

²Department of Bio Chemistry, University of Balochistan, Sariab road Quetta-87300, Pakistan.

³Department of Chemistry, University of Balochistan, Sariab road Quetta-87300, Pakistan.

⁴Department of Statistics, University of Balochistan, Quetta, Pakistan.

sjabeen_phy@yahoo.com*

(Received on 5th January 2011, accepted in revised form 1st November 2011)

Summary: We studied Faujasite type molecular sieves by using Fermi Dirac statistics and the quantum theory of dielectricity. We developed an empirical relationship for quantum capacitance which follows an inverse Gaussian profile in the frequency range of 66Hz – 3MHz. We calculated quantum capacitance, sample crystal momentum, charge quantization and quantized energy of Faujasite type molecular sieves in the frequency range of 0.1 Hz – 10⁴ MHz. Our calculations for diameter of sodalite and super-cages of Faujasite type molecular sieves are in agreement with experimental results reported in this manuscript. We also calculated quantum polarizability, quantized molecular field, orientational polarizability and deformation polarizability by using experimental results of Ligia Frunza et al [13]. The phonons are over damped in the frequency range 0.1Hz – 10 kHz and become a source for producing cages in the Faujasite type molecular sieves. Ion exchange recovery processes occur due to over damped phonon excitations in Faujasite type molecular sieves and with increasing temperatures.

Key words: Charge quantization, Quantum capacitance, Sodalite and super-cages, Quantized molecular field, orientational and deformation polarizabilities, over damped phonon excitations

Introduction

Polarization effects are the assets of dielectrics and of dielectricity. The significant use of polarization is switching and relaxation time to control electronic devices. The quantum response of polarization is the manifestation of GMR (giant magneto resistance), a recent discovery in dielectricity for enhanced storage capacity with charges, by Nobel Prize winners, Albert Peter and Paul Grubber of the year, 2007[1]. Jonscher provided far-reaching analysis of dielectric relaxation in solids [2]. The indispensable component of all dielectric materials is the variation of dielectric parameters with frequency of an applied electric field. Jonscher deciphered descriptive and classical dielectric behavior by using exponent laws [3]. Current literature on dielectric response accent on applications rather than looking into its physics [4-11]. We observed some of the surprising results which are confirmed by considering the microscopic aspects of dielectricity such as “Quantum behavior of dielectricity”[14]. We modified the Clausius Mossotti and Debye equations with our conjecture of charge quantization [14]. We considered the quantum dipole moment as charge quantization (charges are fractionally quantized) but the value of the charge on an electron remained same.

We discovered an idea of charge quantization [14] and deliberated the quantum conductance in dolomite [11] by focusing the

imaginary part of permittivity of dielectricity. We inferred from our model[14] that the induced quantum polarizability of ions or of atoms and of molecules is three times the imaginary part of the permittivity of dielectric material(modified form of Clausius-Mossotti equation). With our conjecture of charge quantization, Lagevin Debye equation is modified which yielded formulas for induced polarization(deformation polarizability) and the other for orientation polarizability. We now use the results of Faujasite – type zeolite [13] and investigated them by applying the “quantum behavior of dielectricity in dolomite” [12]. We performed the quantum mechanical calculations on Faujasite type zeolite [13] by using our research findings [12, 14].

The both X and Y types Faujasite molecular sieves known as sodalite cages have truncated octahedral structures, respectively. The diameter of sodalite cages is 0.66 nm, which is joined by six-membered rings with diameter of 0.2 nm [13]. The hourglass shaped super cage network is formed due to the tetrahedral coordination arrangement of sodalite cages. These super cages are controlled by the interjoined 12-membered rings, whose diameter is 0.74nm [13].

Our investigations [12, 14, 15-17] are relevant to dig out some quantum mechanical behavior connected with ions, atoms or molecules

*To whom all correspondence should be addressed.

and are verified with new calculations performed in this manuscript. We introduced an analysis for the comparison of the sizes of cages in this manuscript by using solid state theory and indeed the Fermi-Dirac statistics [18-21].

Results and Discussions

We used the experimental results of Ligia Frunza, Hendrik Kosslick, Stefan Frunza and Andreas Schonhals [13] and performed calculations by using quantum statistics (Fermi Dirac statistics) [18] and our newly developed “quantum theory of dielectrics”, only in the frequency range of 66Hz~3MHz. We also studied quantum capacitance in the frequency range 0.1Hz – 10⁴ MHz.

We accomplished the new findings on results of Faujasite–Type zeolite [13]. We consider the imaginary part of permittivity at different temperatures, .i.e., 254-303K and in the frequency range 0.01-10⁹ Hz as shown in fig. 1 [13]. We performed the quantum mechanical calculations based on our newly developed quantum theory of dielectricity [14].

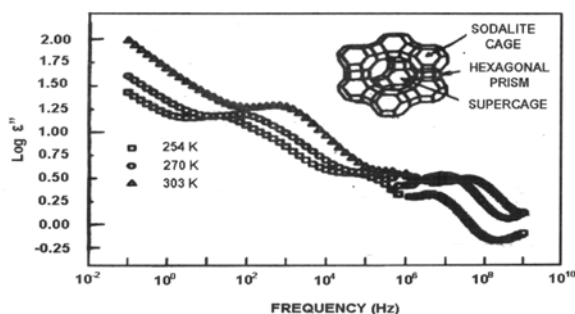


Fig. 1: Results are reproduced from Ligia Frunza, Hendrik Kosslick, Stefan Frunza and Andreas Schonhals “Unusual Relaxation of water inside the Sodalite cages of Faujasite-Type Molecular Sieves”, Journal of physical chemistry B, vol.106, No.36, 9192-9194 (2002).

(Table-1, 2) shows results on Deby velocity, Deby temperature, Deby wave vector, Deby-wave length, Fermi wave vector and Fermi wave length. Deby wavelengths correspond to phonon excitations. Fermi wavelengths decide about occupancy level and indeed about dispersion relationship (E verses k) due to which characteristic structures are formed. We used the well established formulas of Fermi Dirac statistics in table- 1 and 2 by considering our interpretations and indeed calculations [18]. Our calculations confirm $k_F \ll k_D$ and are evident in (Table-1, 2). This shows the absence of s-d interaction. This is why λ_F is considered equivalent to

radius of super cage while λ_D for radius of sodalite cages. We calculated diameter of sodalite cages by using Deby wavelength, .i.e., $2\lambda_D$ and diameter of super cage by using Fermi wavelength, .i.e., $2\lambda_F$, respectively by using quantum statistics (Fermi Dirac statistics). We calculated atomic concentration of Na₅₈(AlO₂)₅₈(SiO₂)₁₃₆mH₂O by taking the atomic concentration of Na, Al and Si [19] and used the procedure mentioned in one of our research paper [18].

Table–1: shows calculations for Deby velocity, Deby temp, Deby wave vector, Deby wavelength, diameter of Sodalite cage.

Sample Zeolite NaY

S.NO	Parameter's Formula's	VALUE
1	Deby Velocity, m/sec	5.6×E 4 m/ sec
	$v_D = \frac{\omega_D}{\left(6\pi^2 \frac{N}{V}\right)^{\frac{1}{3}}}$	
2	Deby Temperature, K	980K
	$\Theta_{\text{Theor}} = \frac{h v_D}{k} \left[\frac{6\pi^2 N}{V} \right]^{\frac{1}{3}}$	
3	Deby wave vector, m-1	1.77× E 10m-1
	$k_D = \left(\frac{6\pi^2 N}{V} \right)^{\frac{1}{3}}$	
4	Deby wave length, m	0.35n m
	$\lambda_D = \frac{2\pi}{k_D}$	
5	Diameter of Sodalite cage, m	0.7 n m
	$D_d = 2\lambda_D$	

Table–2: shows calculations for Volume of Sodalite cage, Fermi wave vector, Fermi wave length, Diameter of Super cage, Volume of Super cage.

Sample Zeolite NaY

S.NO	Parameter's Formula's	VALUE
6	Volume of Sodalite cage, m ³	1.8 × 10-28 m ³
	$V_D = \frac{4}{3} \pi r_D^3$	
7	Fermi wave vector, m-1	1.4 × E 10 m-1
	$k_F = \left(29.60 \frac{N}{V} \right)^{\frac{1}{3}}$	
8	Fermi wave length, m	0.45 nm
	$\lambda_F = \frac{2\pi}{k_F}$	
9	Diameter of Super cage, m	0.9 nm
	$D_F = 2\lambda_F$	
10	Volume of Super cage, m ³	3.8× E-28 m ³
	$V_F = \frac{4}{3} \pi r_F^3$	

Atomic concentration =

$$[(58 \times 2.652) + (58 \times 6.02) + (136 \times 5)] / (58 + 58 + 136) (3) = 1.565 \times 10^{28} \text{ m}^{-3}$$

N/V is obtained by multiplying the valency by atomic concentration

$$\begin{aligned} N/V &= 6 \times 1.565 \times 10^{28} \text{ m}^{-3} \\ N/V &= 9.4 \times 10^{28} \text{ m}^{-3} \end{aligned}$$

We used the formulas given in Table-1 following the calculations [19] which are based on Fermi Dirac statistics. Our theoretical results for diameter of sodalite and super-cage are in conformity with the experimental results [13].

Our calculations for diameter of sodalite and super-cage, respectively show that phonons excite ions to develop a cage. The imaginary part of permittivity with frequency range 0.1Hz-5000 MHz at three different temperatures 254K, 270K and 303K are shown in (Fig 2, 3, 4) respectively. We select peak and asymptotic frequencies at 254K, 270K and 303K, respectively and performed quantum mechanical calculations summarized in Table-3 and Table-4.

Fazl Ur Rahman, Syed M Raza and Muhammad A Ahmed found newly developed formulas [14] as shown in Table-4 to account for the quantum behavior of dielectrics and dielectricity. Let us give a brief summary of these formulas. They modified the Clausius Mossotti equation for dielectricity [20] by considering our hypothesis on charge quantization [12]. The modified form of Clausius Mossotti equation is

$$\alpha_q = 3\varepsilon'' \quad (1)$$

where α_q stands for quantum polarizability and ε'' is the permittivity of the dielectric material. Remember that α_q is defined at the molecular or atomic level. They obtained the molecular electric field by dividing the quantum mechanical dipole moment, .i.e., (charge quantization) with quantum polarizability, .i.e.,

$$E_m = \frac{hQ}{\alpha_q} \quad (2)$$

where h is planks constant and Q is the quantum charge. Remember that the value or magnitude of charge remains same but is fractionally quantized. With Langevin – Debye equation [20], they obtained modified relationships for orientation and deformation polarizabilities, respectively, .i.e.,

$$\alpha_{\text{orientation}} = \frac{h^2 Q^2}{3kT} \rightarrow (3)$$

where k is the Boltzman constant and T the temperature in kelvin.

$$\alpha_q = 6h\varepsilon'' R_0^3 \rightarrow (4)$$

where ε'' is the imaginary permittivity and R_0 is the ionic length between ions. We used radii of Al ions as ionic length, .i.e., 0.72×10^{-10} m [20]. The Table-3 shows that the wave length is constant at lower peak frequencies with given increasing temperature. The quantum mechanical momentum is analogous to charge quantization. The quantum capacitance is rapidly increasing with the increasing temperature. The charge quantization is increasing rapidly with increasing temperature. At the lower frequency the charge quantization is also increasing with increasing temperature. At the high peak frequency the charge quantization almost remains constant with increasing temperature. At the lower asymptotic frequencies f_a the charge quantization is increasing with increasing frequency and temperature. For the upper asymptotic frequency f_b the charge quantization almost remains constant for 254-270K while at 303K the charge quantization increased.

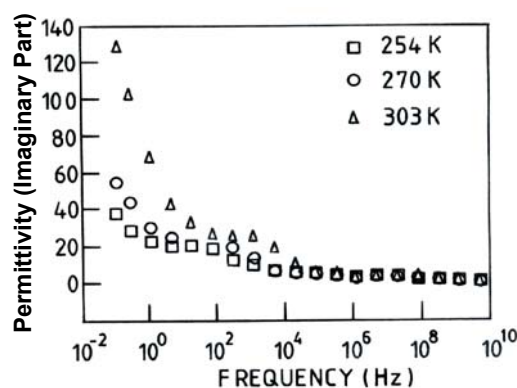


Fig. 2: shows permittivity (Imaginary part) at 254K, 270K and 303K.

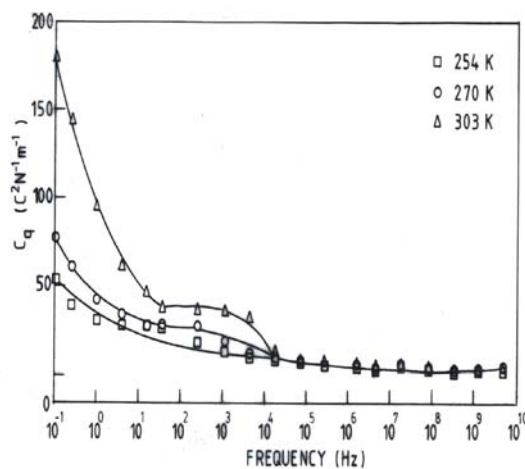


Fig. 3: shows quantum capacitance at 254K, 270K and 303K.

Table-3 shows calculations for wavelength, quantum capacitance, charge, sample crystal momentum, quantum dipole moment and energy at peak and asymptotic frequencies (maximum and minimum turning points).

TempK	S. NO	Peak freq f_p (Hz)	Wave length, λ , m	C_{quan} , Farad	$Q=CV \times 10^3, C$	$p = h/\lambda, \text{JHz}^{-1}\text{m}^{-1}$	$d_{\text{quan}} = hQ_{\text{quan}} / \text{Js}$	$E = hf, \text{eV}$
254	1	0.1 Hz	30×10^8	38	9.1	7.95×10^{-42}	2.2×10^{-28}	23.85×10^{-34}
	2	16 Hz	0.2×10^8	20.5	4.9	1.19×10^{-39}	1.2×10^{-28}	38.17×10^{-32}
	f_a	1 Hz	3×10^8	23	5.5	7.95×10^{-41}	1.3×10^{-28}	23.85×10^{-33}
270	f_b	$4 \times 10^3 \text{ Hz}$	6.9×10^4	7	1.7	3.45×10^{-37}	0.4×10^{-28}	95.42×10^{-36}
	1	0.1 Hz	30×10^8	55.5	13	7.95×10^{-42}	3.2×10^{-28}	23.85×10^{-34}
	2	66 Hz	0.045×10^8	21	5	5.3×10^{-39}	1.2×10^{-28}	15.74×10^{-31}
	3	$11.8 \times 10^6 \text{ Hz}$	30	5	1.2	7.95×10^{-34}	0.3×10^{-28}	28.15×10^{-38}
	f_a	1 Hz	3×10^8	31	7.4	7.95×10^{-41}	1.8×10^{-28}	23.85×10^{-33}
303	f_b	$4 \times 10^3 \text{ Hz}$	7×10^4	9	2.2	34.1×10^{-38}	0.5×10^{-28}	15.74×10^{-36}
	1	0.1 Hz	30×10^8	129	30.1	7.95×10^{-42}	7.3×10^{-28}	23.85×10^{-34}
	2	$1 \times 10^3 \text{ Hz}$	3×10^5	26	6.2	7.95×10^{-38}	1.5×10^{-28}	23.85×10^{-33}
	f_a	4 Hz	0.75×10^8	44	10.6	3.18×10^{-40}	2.5×10^{-28}	95.42×10^{-33}
	f_b	$4 \times 10^3 \text{ Hz}$	6.93×10^4	19	4.6	3.45×10^{-37}	1.1×10^{-28}	95.42×10^{-36}

where f_a and f_b corresponds to asymptotic responses of imaginary part of permittivity at different frequencies

Table-4: shows calculations for semi quantum polarizability, quantized molecular field, and orientation polarizability, deformation polarizability at peak frequencies 254K, 270K and 303K.

Temp. (K)	S.NO	Peak frequency f_p (Hz)	Semi quantum polarizability $\alpha_q = 3\epsilon''$ ($\text{C}^2\text{N}^{-1}\text{m}^{-2}$)	Quantized Molecular field $E_m = hQ/\alpha_q$ ($\text{JNm}^{-1}\text{s}^{-1}$)	Orientational polarizability $\alpha_{\text{orient}} = h^2 Q^2 / 3kT$ (JC^2s^2)	Deformation polarizability $\alpha_d = 6h\epsilon'' R_0^3 / \text{JsC}^2\text{N}^{-1}$
254	1	0.1	114	19E-34	1.04E-37	21751E-64
	2	16	61.5	19E-34	3.11E-18	11734E-64
	f_a	1	69	19E-34	3.65E33	13156E-64
270	f_b	$4 \times 10^3 \text{ Hz}$	21	19E-34	3.46E-27	4004E-64
	1	0.1	166.5	19E-34	2.08E-37	31746E-64
	2	66	63	19E-34	2.93E-28	12012E-64
	3	$11.8 \times 10^6 \text{ Hz}$	15	19E-34	1.83E-39	2860E-64
	f_a	1	93	19E-34	6.58E-39	17732E-64
303	f_b	$4 \times 10^3 \text{ Hz}$	27	19E-34	5.08E-39	5148E-64
	1	0.1	387	19E-34	9.65E-37	73788E-64
	2	$1 \times 10^3 \text{ Hz}$	78	19E-34	4.07E-38	14872E-64
	f_a	4	132	19E-34	1.13E-37	25168E-64
	f_b	$4 \times 10^3 \text{ Hz}$	57	19E-34	2.19E-38	10868E-64

where f_a , f_b corresponds to asymptotic responses of ϵ'' at different frequencies

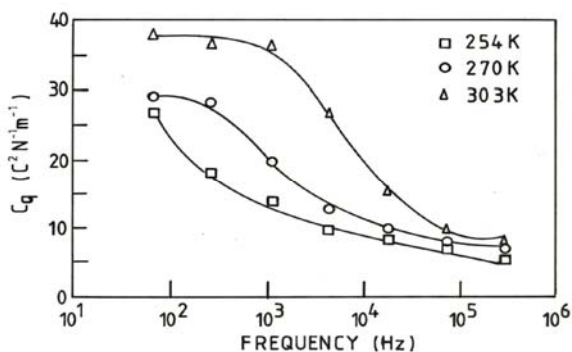


Fig. 4: shows quantum capacitance on semi log paper at 254K, 270K and 303K as envisaged by our theory [14].

The energy E remains constant at lower peak frequency with increasing temperature. At the upper peak frequencies, it is decreasing in the temperature range of 254-270K and then increasing from 270-303K. The energy E appears same at asymptotic frequency f_a with increasing temperature from 254-270K, while at f_b it appears same in the temperature range 270-303K. The energy at f_a

decreases in the temperature range 270-300K. The Table-4 provides the information on quantum polarizability, quantized molecular field, orientation polarizability and deformation polarizability at different temperatures, peak and asymptotic frequencies. The quantum polarizability is three times of the imaginary part of permittivity and increasing with increasing temperature for the smallest value of peak frequency while at relatively high frequencies its value is small as compared to the value at the smallest peak frequency, but is increasing with increasing temperature. At the same time its value is very small for very high frequencies at 270K. For the lower asymptotic frequency its value is increasing with the increasing temperature while at the upper asymptotic frequency its value is small as compared to the value at lower asymptotic frequency, but is increasing with the increasing temperature.

The ratio of the charge quantization to the semi quantum polarizability gives quantized molecular field. To our surprise its value appears constant for all peak and asymptotic frequencies within the temperature range of 254-303K. The orientational polarizability is increasing with the

increasing temperature for smallest value of peak frequency while at the relatively high frequency its value is decreasing with increasing temperature. The orientation polarizability is maximum at the lower asymptotic frequency and at 254K, while for other lower asymptotic frequencies with increasing temperature its value is very small. Its value at upper asymptotic frequencies with increasing temperature is decreasing. The deformation polarizability as shown in Table-4 is increasing with the increasing temperature for the smallest value of peak frequency. At the relatively high frequencies its value is increasing with increasing temperature. For the lower asymptotic value its value is increasing with increasing temperature. Same response is observed for upper asymptotic values. Fig. 3 shows response of over damped phonons in the frequency range of 0.1 Hz to 10kHz. At 303K dynamic recovery of ions for the formation of cages in Faujasite type molecular sieves is evident in the frequency range of 50 Hz to 5 kHz but with constant quantum capacitance.

This means that a new fractional quantum space is configured and that the degenerate fractional quantization is increasing with increasing frequency and temperature. From above discussions we conclude that the complex dielectric response is occurring inside the cavity (volume of molecule or of ionic bonds or of atoms) of material and the cavity is resonating with the natural frequency of the material.

Fig. 4 shows quantum capacitance (C_q), as envisaged by our theory [14] in the frequency range 0.1Hz-5000MHz at 254K, 270K and 303K, respectively. We choose a specific range of frequencies, i.e., 66Hz~3MHz from the results of Ligia Frunza, Hendrik Kosslick, Stefan Frunza and Andreas Schonhals "Unusual Relaxation of Water Inside the Sodalite Cages of Faujasite-Type Molecular Sieves", *Journal of Physical Chemistry B*, vol.106, No.36, 12th Sep, 2002, [13] and plot them on semi log graph paper as shown in fig. 4 at temperatures 254K, 270K and 303K, respectively. The empirical formula for quantum capacitance is suggested which shows an inverse Gaussian behavior. Our theoretical values of quantum capacitance are in conformity with experimental values.

The empirical formula for quantum capacitance is:

$$C_q \propto \exp\left\{-\left(\frac{h\nu}{kT}\right)^2\right\}$$

$$C_q = C_{q_0} \exp\left\{-\left(\frac{h\nu}{kT}\right)^2\right\}$$

where C_{q_0} = Characteristic quantum capacitance at $\nu = 0$, ν the frequency, h the Planck's constant and k the Boltzman constant.

Conclusions

We infer the following conclusions.

1. The quantum capacitance follows the inverse Gaussian behavior as found from experimental results [13] and from our conjecture on charge quantization.
2. The quantum response of polarization is the manifestation of GMR (giant magneto resistance) [1] as is evidenced from our recently developed theory [14].
3. Our calculations for sodalite and super-cage confirm the fact that phonon excite ions to develop a cage and that our theoretical results are in conformity with experimental results [13].

Acknowledgments

We are thankful to Mr. Fazlur Rehman for providing us theoretical research papers [14] and useful discussions.

References

1. A. Peter and P. Gruebber "Giant Magneto Resistance" APS News Letter, (2007).
2. Jonscher, "Dielectric Relaxation in Solids" *Chelsea Dielectric Press*, London (1983).
3. Jonscher, *Nature*, **253**, 717 (1975).
4. D. J. Kim *et al.*, *Journal of Applied Physics*, **93**, 1697 (2003).
5. Fu and Chen, *Journal of Applied Physics*, **93**, 2140 (2003).
6. J Han, *Journal of Applied Physics*, **93**, 4097 (2003).
7. Holten and Kliem, *Journal of Applied Physics*, **93**, 1684 (2003).
8. Brassard and E. I Khakani, *Journal of Applied Physics*, **93**, 4066 (2003).
9. Priya and Uchino, *Journal of Applied Physics*, **91**, 4515 (2002).
10. X. Wang and H. Chen, *Journal of Applied Physics*, **91**, 5979 (2002).
11. Santos, *Journal of Applied Physics*, **92**, 3251 (2002).
12. M. Gormani, Fazl-ur-Rehman, M. A. Ahmed and S. M. Raza, " *Journal of the Chemical Society of Pakistan*, **28**, 414 (2006).
13. F. Ligia, H. kosslick, S. Frunza, and A. schonhals, *Journal of Physical Chemistry B*, **36**, 9192 (2002).
14. F. Rehman, M. A. Ahmed and S. M. Raza, *Science International*, **21**, 29 (2009).

15. Sammina T. Y. Azeemi and S. M. Raza, *Journal of Evidence Based Complementary and Alternative Medicine*, **2**, 481 (2005).
16. S. Jabeen, S. M. Raza, K. Mehmood, S. Atiq and Zia-ul-haq Farooqi, *Journal of the Chemical Society of Pakistan*, **2**, 3 (2009)
17. S. Jabeen, S. M. Raza and G. Vanhoyland, *Journal of the Chemical Society of Pakistan*, **30**, 192 (2008).
18. A. M. Gormani, S. M. Raza, N. Farooqi and M. A. Ahmed. *Solid State Communications*, **95**, 329 (1995).
19. C. Kittel 'Solid State Physics' 8/e John, Wiley & Sons, (2005).
20. O. H. Birel, C. Zafer, H. Dincalp, B. Aydin and M. Can, *Journal of the Chemical Society of Pakistan*, **33**, 562 (2011).
21. O. Hakli-Birel, H. Dincalp, C. Zafer, S. Demic, K. Colladet, D. Vanderzande, Y. Yurum and S. Icli, *Journal of the Chemical Society of Pakistan*, **33**, 403 (2011).